

Watermarking Algorithm Based on a Human Visual Model

J.F. Delaigle^a C. De Vleeschouwer^{a,1} B. Macq^a

^a*Laboratoire de Télécommunications et Télédétection
Université catholique de Louvain
Bâtiment Stévin - 2, place du Levant
B-1348 Louvain-la-Neuve
Tel.: +32 10 47.41.05 - Fax.: +32 10 47.20.89
E-mail: {delaigle, devlees}@tele.ucl.ac.be*

Abstract

This paper presents an additive watermarking technique for grey scale pictures. It consists in secretly embedding copyright information (a binary code) into the picture without degrading its quality. Those bits are encoded through the phase of Maximal Length Sequences (MLS). MLS are binary sequences with good correlation properties. The result of the autocorrelation is much greater than crosscorrelations, i.e. correlations made with shifted versions of this sequence. The embedded bits are retrieved from the result of the correlations. The core of the embedding process is underlaid by a masking criterion that guarantees the invisibility of the watermark. It is combined with an edge and texture discrimination to determine the embedding level of the MLS, whose bits are actually spread over 32 by 8 pixel blocks. Eventually, some results are presented, which analyze the efficiency of the retrieval as well as the resistance of the watermark to compression and its robustness against malevolent manipulation.

Key words: Copyright, Digital Picture Watermarking, Human Vision System Model, Masking, Spread Spectrum.

1 Introduction

Copyright offers protection for the contents of exchanges which take place on the networks. With the development of the Information Society, it is expected

¹ Supported by the Belgian NSF.

that more and more intellectual property and other protected material will be carried on the Superhighway. It is clear that with increasing digitization, classical legal protection is not sufficient but the development of technical protection tools will be the key to the viability of the Information Society. Indeed, the acceptance of new digital audiovisual services depends on whether suitable techniques for the protection of the content providers' interests are available [1].

As a matter of fact, its very viability is threatened by the nature of digital media. First, the replication of digital material is very easy and, more dangerous, is virtually perfect. The copy is identical to the original. The ease of transmission and multiple uses is worrying too. Once a single unauthorized copy has been made, it is instantaneously accessible to anyone who wants it, without any control by the owner of the original content. In fact, the plasticity of digital media is a great menace. Any malevolent user (*a pirate*) can modify any image at will. Such manipulations are really easy with the existing image processing tools, and defy many copyright protection methods.

Fortunately, the digitization of audiovisual contents offers new possibilities for the development of copyright protection techniques. Watermarking is just one. The principle of watermarking is the robust embedding of copyright information (e.g. time and date, Copyright Identifiers) into a given content. This content may be a text [2] [3], an audio content [4], but most often watermarking is applied to still or moving images. This paper will focus on image watermarking for still pictures (extension to moving pictures is possible by independently watermarking some of the pictures of the sequence).

Many laboratories and companies have already developed their own watermarking techniques for digital images. Most of them work directly on the luminance with or without taking considerations about the quality of the watermarked image into account [5,6]. It is also interesting to consider the image content as a channel that can convey a certain amount of information. Different techniques use this approach to embed a copyright code by means of the spread-spectrum theory [7]. Finally, other authors apply their watermarking techniques not on the picture itself but on some of its characteristics, like DCT coefficients [8], fractal coefficients or motion estimation vectors, high resolution coefficients in case of multiresolution encoding [9], or the phase of DFT coefficients [10].

These techniques give different results with different degrees of quality, but all have in common that they have to realize a good trade-off between the robustness of the watermarking, the quality of the watermarked picture and the computational cost. However, only some analyze the quality of the resulting image or use a human visual model to guarantee the invisibility of the embedding [11]. The method presented in this paper also exploits this human

visual model. Yet it is computationally simpler. Moreover, its objective is the hiding of a secret message into the images while the other had been conceived to answer to the simple binary question: "Does the image contain a defined watermark or not?". Of course, these two functionalities are complementary and should be combined in the automated monitoring of copyrighted material on audiovisual networks.

Another asset is the fact that the retrieval of the embedded copyright information does not require the use of the original picture, so that no human intervention is needed for the retrieval of the watermark. This advantage is essential in the use of watermarking for the automated monitoring of audiovisual networks. As a matter of fact, this monitoring permits the automatic detection of copyright violations. This is fundamental given the practical situation, where Copyright Owners possess many copyrighted works and their material is distributed over and over through increasingly developing networks.

2 Perceptive model

The goal of image watermarking techniques is to embed information in the picture content. In the case of an invisible watermark, the watermark must be hidden (*i.e. masked*) by the picture it is inlaid in. The question of embedding visible watermarks is completely different and is addressed by other authors [12]. The watermarking method presented in this paper refers to a masking criterion deduced from physiological and psychophysical studies [13].

2.1 Eye functioning and Masking Concept

It is now admitted that the retina of the eye splits the visual stimulus composing an image into several components. These components circulate by different tuned channels from the eye to the cortex, each channel being tuned to a component. The characteristics of a component are:

- location in the visual field (in the image).
- spatial frequency (in the Fourier domain: the amplitude in polar coordinates).
- orientation (in the Fourier domain: the phase in polar coordinates)

A perceptive channel can only be stimulated by a component of a signal whose characteristics are tuned to its own characteristics. Components that have different characteristics are independent. Moreover, according to the perceptive model of human vision [14], signals that have similar components use the same channels from the eye to the cortex. It appears that such signals interact

and are subject to non-linear effects. *Masking* is one of those effects. It occurs when the *detection threshold*, i.e. *the minimum level below which a signal can not be seen*, is increased because of the presence of another signal. In other words, masking occurs when a signal can not be seen because of another signal with near characteristics but at a higher level.

2.2 The masking model

With the aim of making a model of the masking phenomenon, tests have been done on monochromatic signals, also called *gratings*, i.e. signals of one single frequency and one orientation (f_0, θ_0) . It appears that the eye is sensitive to the contrast of those gratings. L being the luminance, this contrast is defined by:

$$C = \frac{2(L_{max} - L_{min})}{L_{max} + L_{min}} \quad (1)$$

The detection threshold contrast C_s of a test signal is a non linear function of the contrast C_m of a masking signal. When the two gratings have the same frequency and orientation (f_0, θ_0) , this threshold can be expressed as [15]:

$$C_{s_{(f_0, \theta_0)}}(C_m) = \max[C_0, C_0 \left(\frac{C_m}{C_0}\right)^\epsilon] \quad (2)$$

where C_0 is the visibility threshold without a masking effect and ϵ depends on (f_0, θ_0) , typically, $0.6 \leq \epsilon \leq 1.1$.

It is possible to extend that expression to introduce the frequency and orientation dependences. Actually, the masking phenomenon decreases as the couple (f, θ) of the test (or masked) signal differs from the couple (f_0, θ_0) of the masking signal [14]. The general expression of the detection threshold contrast C_s becomes:

$$C_s(C_m, f, \theta) = C_0 + k_{(f_0, \theta_0)}(f, \theta)[C_{s_{(f_0, \theta_0)}}(C_m) - C_0] \quad (3)$$

where:

$$k_{(f_0, \theta_0)}(f, \theta) = \exp\left[-\left(\frac{\log^2\left(\frac{f}{f_0}\right)}{F^2(f_0)} + \frac{(\theta - \theta_0)^2}{\Theta^2(f_0)}\right)\right] \quad (4)$$

In this expression, $F(f_0)$ and $\Theta(f_0)$ are parameters that represent the spreading of the Gaussian function, C_0 is often negligible. The spread of the Gaussian

function depends on the frequency f_0 . The spatial frequency typical bandwidths at half response are 2.5 octaves at 1 c/d and 1.5 octaves at 16 c/d with a linear decrease between these two frequencies [16]. The orientation bandwidth at half response depends on f_0 and takes typical values like 30 degrees at 1 c/d and 15 degrees at 16 c/d [17].

These values fit with other physiological findings that have shown that the spatial frequency bandwidths of the cortex cells range from 0.5 to 2.5 octaves, clustering around 1.2 octaves [18,19] and 1.5 octaves [20]. In these works, the cortex cells behavior is approximated through a Gaussian filter with an elliptical envelop whose axis is parallel to the orientation feature of the cell. It has been established that the aspect ratio of the envelope is 1.5-2 [20,21]. It is easy to check that this is in accordance with the 30 degrees half bandwidth along θ .

According to the same expression, the frequency dependence of the detection threshold has a Gaussian form. Only near frequency signals can interact. When the frequency of the masking signal (the mask) is far from that of the signal to mask, the detection threshold is almost equal to C_0 .

2.3 The masking criterion

It is important to notice that these results only concern gratings signals. To deduce a masking criterion that applies to signals such as real images, the preceding masking condition has to be adapted. So, it is necessary to define a new concept able to take the place of the contrast and defined for real images. This new concept [13] is called *local energy* [22].

Local energy is defined on narrow band signals. **The local energy of a narrow band signal corresponds to the square of the amplitude of the signal envelope.** In the framework of the analytic representation of signals, in which signals are only described by positive frequencies, the local energy is the square modulus of the local signal complex value.

A picture is a broadband signal. The contrast related to a particular frequency and orientation is the local energy of the narrow band signal resulting from the filtering of the original picture by the **Gabor filter** (see equation (5)) whose characteristics are tuned to the perceptive component under consideration. Actually, this filter was chosen to model human perception. Its effect is close to the filtering effect of the visual cortex cells. As a conclusion, local energy is calculated according to the scheme presented in the next figure:

Having introduced this local energy concept, **the masking criterion** can be defined:

“A noise is masked by a mask if $\forall pixel (x, y)$ and $\forall(f_0, \theta_0)$, $E_{mask,(f_0,\theta_0)}(x, y) \geq E_{noise,(f_0,\theta_0)}(x, y)$ ”.

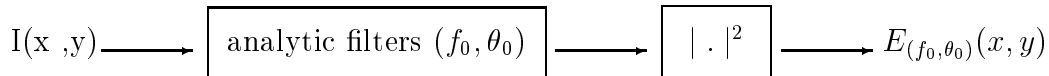


Fig. 1. Local energy computation.

Of course, in practice, the Fourier frequency and phase space (f_0, θ_0) has to be sampled. This generates a bank of filters whose central frequencies correspond to independent components spread all over the Fourier space. It is widely accepted [16,21] that 4 or 5 frequencies and 4 to 9 orientations are sufficient. The standard choice is twenty filters (5 frequencies and 4 orientations). Recently, Tai Sing Lee, by extending to two dimensions the frame criterion developed by Daubechies [23], has derived the conditions under which a set of continuous 2D Gabor wavelets provides a complete representation of any image [24]. He has proved that 2D Gabor wavelets with a 1.5 octave bandwidth guarantee a complete representation, but only if the number of sampling orientations is above 6. Noting that the bandwidth of the filters we have used is slightly greater than 1.5 octave, this result also tends to prove that the 20 sampled filters efficiently cover the Fourier space.

2.4 Perceptive filter in the horizontal direction

In the Fourier space, analytic filters used to extract local energy are defined by:

$$G_{(f_0, \theta_0)}(f, \theta) = \exp\left[-\left(\frac{\log^2\left(\frac{f}{f_0}\right)}{F^2(f_0)} + \frac{(\theta - \theta_0)^2}{\Theta^2(f_0)}\right)\right] \quad (5)$$

The embedding process presented in section 3.1 explains that the watermark is limited to one horizontal perceptive component. So, in the following, only horizontal filters will be useful (i.e. $\theta_0 = 0$). Moreover, as explained in section 2.3, it is not necessary to verify the masking criterion $\forall(f_0, \theta_0)$ included in this perceptive component centered around (f_0, θ_0) . The study of the perceptive energy at (f_0, θ_0) is sufficient.

If u and v designate horizontal and vertical frequencies (i.e. corresponding to x and y directions), if u_0 is the central horizontal frequency and if the filter is narrow-band according to u and v frequencies, appropriate Gabor analytic

filters can be approximated by the following separable filters:

$$G_{u_0}(u, v) = \exp\left[-\left(\frac{\log^2\left(\frac{u}{u_0}\right)}{F^2(u_0)}\right)\right] \cdot \exp\left[-\left(\frac{v}{u_0 \cdot \Theta(u_0)}\right)^2\right] = G_{1,u_0}(u) \cdot G_{2,u_0}(v) \quad (6)$$

Making the common hypothesis that the observer is located at a distance equal to 6 times the picture height, *cycles/degree* frequencies can be converted into normalized ones (f_{norm}) according to the sampling frequency. Indeed, N being the number of columns of the picture (i.e. number of pixels in one line),

$$f_{norm}\left(\frac{\text{cycles/screen}}{\text{Number of pels}}\right) = \frac{f(\text{cycles/degree}) \times 9.53(\text{degrees/screen})}{N(\text{Number of pels})} \quad (7)$$

As the sampling rate is the same in both horizontal and vertical directions, the normalization factor $\frac{9.53}{N}$ is also valid to convert *cycles/degree* horizontal frequencies into normalized frequencies. So, according to the above considerations about the bandwidth of the filter defined by equation (4), $F(u_0)$ and $\Theta(u_0)$ in equation (6), u_0 being a normalized frequency, are defined in terms of normalized frequencies as:

$$F(u_0) = \frac{\frac{-1}{15} \cdot \left(\frac{u_0 \cdot N}{9.53} - 1\right) + 2.5}{2 \sqrt{\ln(2)}} \quad (8)$$

$$\Theta(u_0) = \frac{31 - \frac{u_0 \cdot N}{9.53}}{\sqrt{\ln(2)}} \quad (9)$$

In the spatial domain (x, y) , the inverse Fourier transform of $G_{u_0}(u, v)$ is $g_{u_0}(x, y) = g_{1,u_0}(x) \cdot g_{2,u_0}(y)$. For each pixel, the local energy is computed as the square of the module of the complex number obtained by convolving this filter with the picture. In section 3.1.2, it is explained that the normalized frequency of the filters used is located around 0.15 for 512×512 pictures. It is added that, as the reference inscription frequency is expressed in *cycles/degree* (8 *cycles/degree*), the value $u_0 \cdot N$ is independent of picture size (N).

After generating the $g_{1,u_0}(x)$ and $g_{2,u_0}(y)$ filters around this frequency, it is possible to make the following statements:

- If $g_{1,u_0}(x)$ is computed by inversion of the Discrete Fourier Transform (DFT) obtained by sampling $G_{1,u_0}(u)$, it is obvious that a few samples are sufficient to have a good approximation of the ideal filter. Figure 2 shows the real and imaginary part of the g_1 analytic filter. It also shows, in the Fourier domain, the G_1 filter resulting from a 9 samples approximation. In the following, this

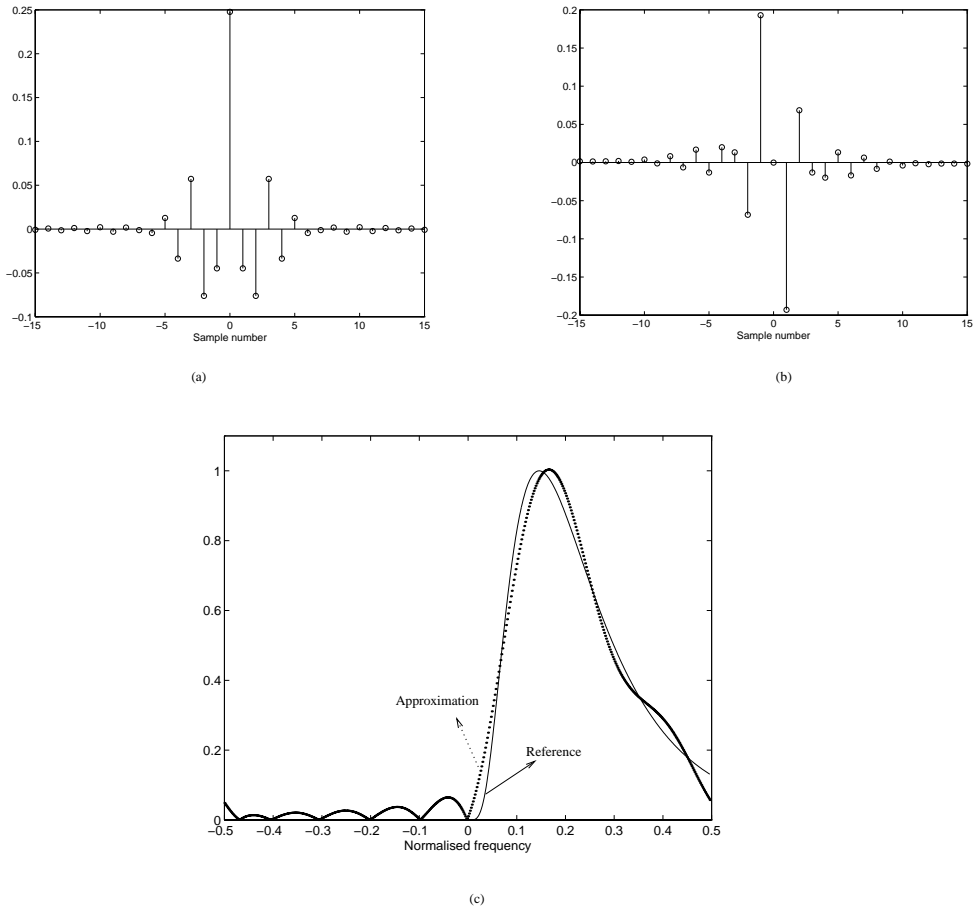


Fig. 2. Horizontal factor (g_1) of the perceptive analytic filter ($u_0.N = 0.15.N$): (a) real part in the spatial domain, (b) imaginary part in the spatial domain, (c) Fourier transform of the approximation using 9 complex samples.

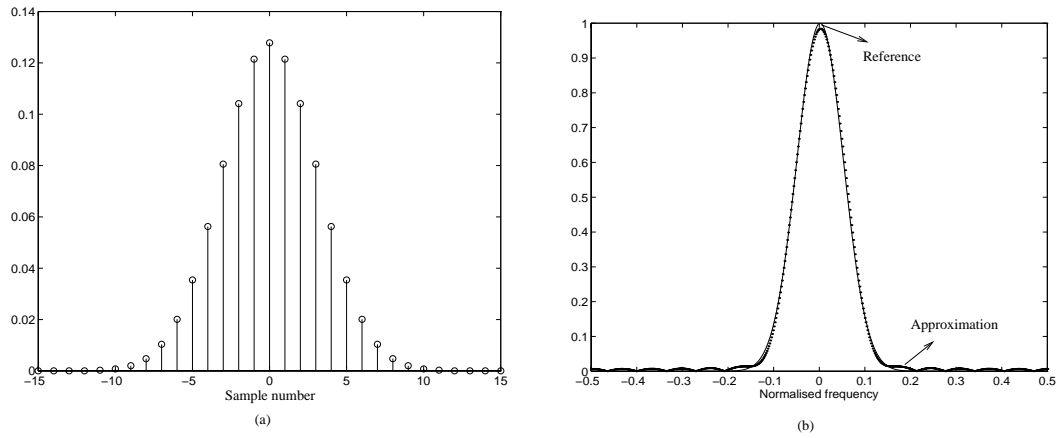


Fig. 3. Vertical factor (g_2) of the perceptive analytic filter ($u_0.N = 0.15.N$): (a) filter actual samples in the spatial domain obtained as the inverse Fourier transform of the reference Gaussian function (see (b) and equation (8)); (b) 15 samples filter approximation.

9 samples complex filter will be used as the horizontal part of the analytic filter.

- $g_{2_{u_0}}(y)$ can be expressed analytically as the inverse Fourier transform of a Gaussian function (equation (10)). Figure 3 shows the filter samples. In the following, the 15 most significant ones will be used to provide a genuine approximation of the filter.

$$g_{2_{u_0}}(y) = \sqrt{\pi} \cdot u_0 \cdot \Theta(u_0) \cdot \exp[-(\pi \cdot y \cdot u_0 \cdot \Theta(u_0))^2] \quad (10)$$

3 Information embedding

3.1 Main Features of the Method

Looked at from the angle of information theory, watermarking is similar to transmitting a bitstream through a very noisy channel, which is the original picture, under the constraint of watermark invisibility. It is with this aim that the embedding process searches for the best trade-off while adjusting the level of the watermark. The method presented in this paper suggests adjusting this level to just below the invisibility threshold. This is done through a local examination of the picture perceptual content. Due to the heaviness of the perceptive filtering, only one component has been chosen, i.e. the horizontal component. This means that this method creates a narrow-band watermark, oriented horizontally. Only one perceptive filtering is needed to verify the masking criterion.

3.1.1 Maximum Length Sequences (MLS): L orthogonal Codewords

As mentioned in section 1, the aim of the proposed algorithm is to permit embedding a secret message (identification code) into images. Interested readers are referred to another paper [11] in which the authors describe a robust method for image authentication, i.e. an answer to the key question whether the image contain sa defined watermark or not.

Due to the invisibility constraint, the level of the watermark has to be below that of the picture. The picture is a noise regarding the retrieval of the transmitted information. This high noise in the transmission channel leads to spread the information bitstream over binary code words. Code words are sequences of 1 and -1 symbols. The decoding of these code words is performed through correlations. This entails the use of orthogonal code words. Besides, equiprobable sequences symbols are advantageous in order to reduce the effect of the noise after correlation.

Maximal Length Sequences (MLS) perfectly fulfill these requirements, since MLS sequences are nearly orthogonal to their shifted versions. Crosscorrelations between shifted versions are equal to -1, whereas autocorrelations are equal to the length of the MLS sequence. They are also referred to as pseudo-random sequences, because the various statistics associated with the symbols occurrences are close to those associated with coin-toss sequences [25]. MLS exist for all integer values n , with a period $L = 2^n - 1$, and can be easily generated by proper connections of feedback paths in an n -stage shift register circuit [26].

In the rest of the paper, the L codewords of the L -ary system are thus shifted versions of a particular MLS. Nearly n bits are coded through the phase, i.e. the number of shifts, of a $L = 2^n - 1$ long sequence. The choice of the length L is the result of a trade off. A long sequence permits a more efficient and reliable decoding. On the other hand, making the sequence longer decreases the number of bits encrusted in the image. A viable compromise is the use of a 31 symbols long sequence, i.e. $n = 5$. So, each time a complete sequence is embedded in the picture, nearly 5 bits of information are transmitted. As every symbol of the MLS is spread over 8×32 pixels rectangles (see section 3.1.2), 512×512 pictures can contain 33 complete MLS. That means that nearly 165 bits are embedded in a 512×512 picture. More accurately, there are 31 possible phases for each MLS, which means 31 possible messages each. This leads to a total information of $\log_2(31^{33}) = 163$ bits.

3.1.2 *Inscription in one Perceptive Component*

Once the basic information has been encoded through the MLS phase, the resulting sequence has to be embedded in the picture. This has to be done in a way that ensures invisibility, undetectability, resistance towards malevolent manipulations and also guarantees adequate retrieval.

The effectiveness of masking concepts for ensuring the invisibility of extra information hidden into a picture has already been proved [11]. These masking concepts have been described in section 2. A major feature of the Human Visual System is the fact that the retina of the eye splits the observed picture into components characterized by their location, spatial frequency and orientation. In order to make a simple use of the masking concepts (see section 3.2), it was decided to excite one single perceptive component at a time. This excited component is horizontal in our case. To generate a signal with spectral components around the central frequency of the excited perceptive channel, the MLS modulates a carrier at this frequency. This frequency changes for each MLS embedded in the picture. The choice of the frequencies is secret in order to make the watermark resistant against piracy. A malevolent user is not able to remove the watermark from the picture without knowing this secret

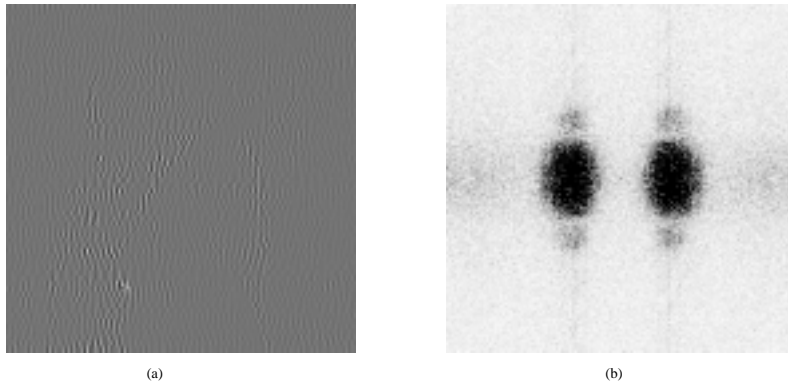


Fig. 4. Lena's watermark: (a) spatial domain, (b) Fourier space.

frequency. **The choice of the possible carriers is limited to the frequencies in the interval $[5, 10]$ cycles/degree**, i.e. to the interval $[0.1, 0.2]$ expressed in normalized frequencies for 512×512 pictures. The perceptive model is less valid and less effective for lower frequencies and the image content does not permit to watermark at a sufficient level for higher frequencies. Moreover, image features at higher frequency are less visible and can be removed without altering the global picture quality. So, a filtering may easily remove the watermark.

The resulting signal has to be narrow band in both vertical and horizontal directions so as to stimulate only one perceptive component (i.e. the horizontal one). This signal is thus filtered in both horizontal and vertical directions. In order to keep the major components of the signal, each symbol of the MLS must be spread over some pixels, actually over a 32×8 rectangle (8 lines of 32 pixels).

In the range of possible carrier frequencies ($[5, 10]$ cycles/degree), the vertical half bandwidth of the perceptive filter is about 3 cycles/degree. According to equation (6), the half bandwidth at half response in vertical direction is $\sqrt{\ln(2)} \cdot \Theta(u_0) \cdot u_0$ where $\Theta(u_0) = (31 - u_0) / (\sqrt{\ln(2)})$. The fundamental harmonic of the watermark in the vertical direction has to be preserved after the vertical filtering limiting the watermark to a single perceptive component. If one binary symbol of the watermark is spread on X lines, this fundamental harmonic is located around $\frac{0.5 \times N}{X \times 9.53}$ cycles/degrees. So, X has to be greater than $\frac{0.5 \times N}{3 \times 9.53}$. This leads to spread one symbol on 8 lines for a 512×512 picture.

Horizontally, each symbol of the MLS is spread over 32 columns. This choice was made for retrieval efficiency purposes (see section 3.1.1) and is sufficient to generate a narrow band watermark.

So, in the proposed implementation, each symbol of the MLS corresponds to an 8-pixels-high and 32-pixels-wide rectangle. Figure 4(b) presents the spectrum (Fourier transform) of an embedded signal, i.e. the watermark evaluated on

the well known picture of “Lena” (see figure 7(a)). The watermark appears to be spread on neighboring perceptive components. So, ideally the masking criterion should be verified for these perceptive components. Nevertheless, as the major part of the watermark is concentrated in the horizontal component, one may admit that, if the invisibility criterion is verified for this component then the watermark should be invisible in the whole picture.

As the inscription is generated on groups of eight lines, during the retrieval, each group of eight lines is also considered as a whole. Figure 5 illustrates the receiver for this L-ary orthogonal codeword signaling. The center frequency of the band pass filtering and the demodulation frequency are adapted to follow the frequency hopping, i.e. the change of the MLS carrier frequency. The knowledge of this frequency hopping is the secret part of the embedding process.

Synchronization is a major problem during decoding, i.e. the acquisition of the MLS phase and the carrier phase. Choosing to bind the carrier phase to the MLS phase reduces these problems to one synchronization. This problem was omitted during the tests since embedding always began at the first column of the digital picture. Nevertheless, in the context of analog video product watermarking, the digitization may be slightly different between coding and decoding. Even in the digital world some lines and columns shifting appear in the professional broadcast chain. So, this problem is crucial in a number of applications. A possible approach would be to include a pattern, typically a number of synchronization bits as part of the watermark. These bits could be located during the first stage of retrieval through the search of a maximum correlation when computing the retrievals with different phases. Once synchronization is achieved, the correlation properties of MLS could be used to compensate for small shifting in the MLS phase, due for example to the loss of a column of the picture.

3.2 Invisibility Requirement

This section describes how to determine the inscription level according to the picture content. A two-stage filtering process has been implemented:

- First, a perceptive analytic filter adapted to the frequency of the MLS carrier is used to estimate the masking capabilities of the picture in the studied area and in the perceptive component in which the MLS is embedded.
- Second, a high frequency filter detects the main features (i.e. the edges) of the picture and, thanks to a spatial morphological filtering, distinguishes between uniform and textured areas to correct the perceptive model imperfections.

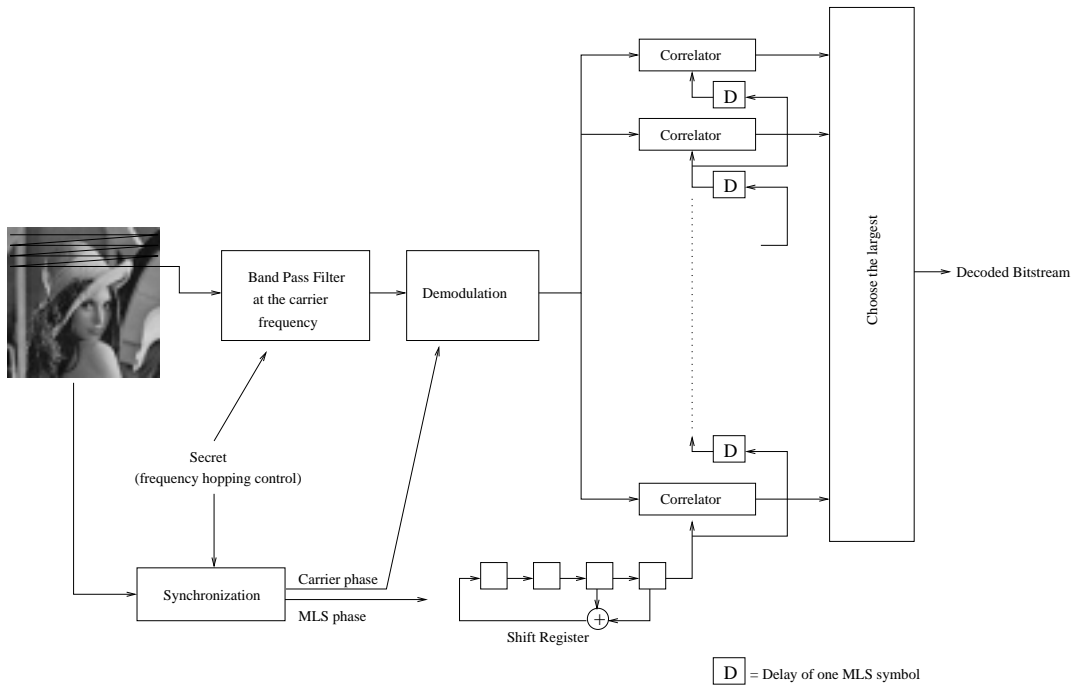


Fig. 5. Retriever for L-ary Orthogonal-Codeword Signaling.

The results of these two filtering processes are then combined to produce an energy level whose square root fixes the local inscription level.

3.2.1 Perceptive Analytic Filtering

The masking criterion (see section 2.3) is strongly simplified when the noise is contained in one single perceptive component. In this case, the noise designates the watermark while the mask corresponds to the original picture. The perceptive component is characterized by its horizontal orientation and by the MLS carrier frequency u_0 . So, the noise -the watermark in our case- is perceptively invisible when added to the mask, i.e. the original image, if $\forall(x, y), E_{mask, u_0}(x, y) \geq E_{noise, u_0}(x, y)$ with E being the local energy defined in section 2.3.

The local energy of the original image is extracted by the analytic filters defined in section 2.4. The local energy of the image formed with the MLS could be extracted in the same way. Nevertheless, due to the small bandwidth of this signal and to the concentration of its spectrum around the central frequency of the perceptive component, it can be assumed that Gabor filtering does not modify the modulated MLS. As a result, the local energy is more or less the square of the local amplitude of the MLS signal.

So, to satisfy the masking criterion, the amplitude $A(x, y)$ of the MLS has to be lower than the local energy of the original picture in the perceptive component centered at the frequency of the carrier

modulated by the MLS. In order to produce a maximal level watermark, the amplitude is chosen equal to the local energy.

3.2.2 Edges and Textures Discrimination

Nevertheless, this simple implementation has a number of drawbacks. In fact, the produced watermark is visible along edges and could be embedded with higher energy in textured regions, i.e. in regions that have great activity.

The problem of visibility reveals some of the weaknesses of the perceptive model. Because of their width (15 pixels), perceptive filters spread the peak of energy near sharp edges on some pixels, leading to the embedding of the watermark in a rather large area around the edges. Specific studies about the masking phenomenon around sharp edges have shown that this phenomenon is strictly local, i.e. it concerns only a very few pixels around the edge [27]. A way out of this problem is to make use of **edge detector filters**. These filters have good spatial location, i.e. they permit to precisely localize sharp edges. The used edge detectors evaluate the envelope of the original signal filtered by a large bandwidth complex filter [28] in the way described in section 2.3, thus it can be considered another kind of local energy. In one dimension, impulse response of the analytic representation of this filter is illustrated on Figure 6 (it is worth noting that the maximal value of the Fourier transform of this filter is 2 and not 1 as for the perceptive filters).

This complex response is $S + j.A$ with

$$S = [0, -0.158, 0.315, -0.158, 0] \quad (11)$$

$$A = [0, -0.158, 0.315, -0.158, 0] \quad (12)$$

In two dimensions, the energy results from the square of the sum of the energy estimated in horizontal and vertical directions. Figure 7 presents the local energy produced by these edge detector filters. Nevertheless, such filters do not discriminate isolated edges from edges in active areas. This is why they are followed by a non linear **morphological filtering** [29]. A *closing* of the edges detector energy increases the energy level between neighboring edges but does not modify it in the surroundings of isolated edges. The *structurant element* size fixes what neighboring edges are. The resulting energy has strong values located on sharp edges and spread on active areas, i.e. areas having a strong edges density.

As a conclusion, the information produced through this edge detector and morphological filtering brings precise information about the location of the picture

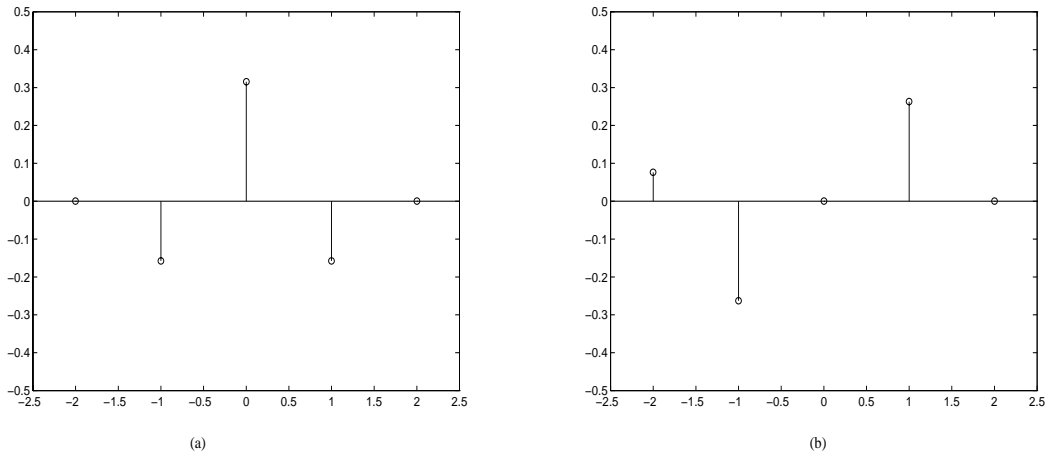


Fig. 6. Real (a) and imaginary (b) part of the samples of the edge detector filter.



Fig. 7. Edge detector filters applied on Lena: (a) Original greyscale picture, (b) Edge detector local energy determined by edge detection (darkness represents high values).

masking features. This permits to correct the result obtained from the perceptive filtering, which provides direct information about the level of inscription allowed in the perceptive component of the carrier frequency but suffers from weak location capabilities. Actually, the MLS amplitude corresponds to the minimum between the perceptive energy and twice the edge detectors energy value (it is worth noticing that both perceptive and edges detector filters have been normalized, i.e. their maximal value in the frequency domain is equal to one). This correction process does not heavily increase the computational cost but permits to reduce the embedding level near isolated edges. The resulting embedding process scheme is illustrated on Figure 8. The watermarked bitstream contains some synchronization bits (see end of section 3.1.2). Some parts of this figure need further explanation. The lowest branch of the scheme evaluates the sign of the original picture contribution in the correlation computation. The sign of the embedded MLS is chosen to increase the absolute value of this contribution. The last band pass filter, coming before the ad-

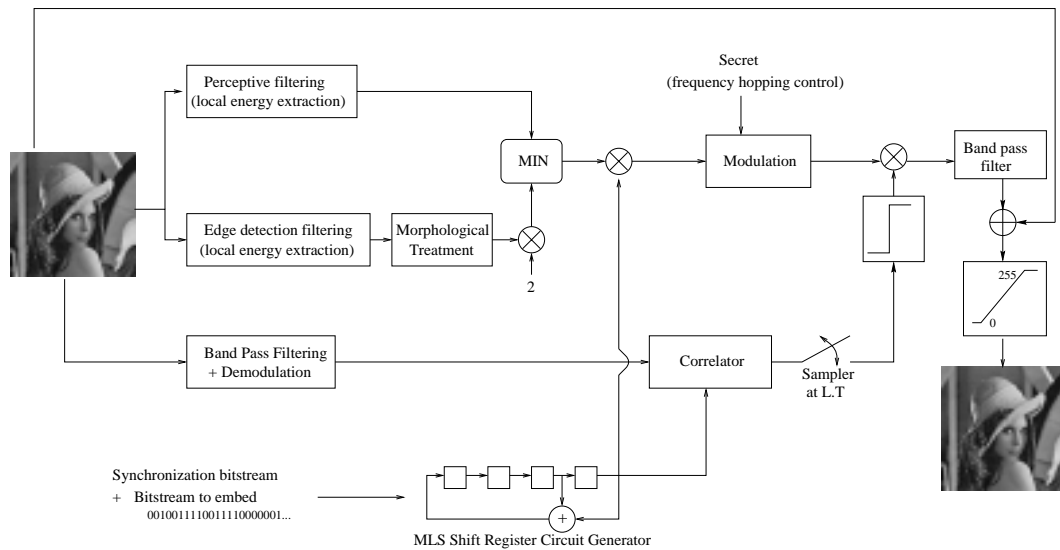


Fig. 8. Watermark embedding process.

dition of the watermark to the original picture, ensures that the embedded signal is really narrow band (see section 3.1.2). Finally, the limiter maintains pixel values between 0 and 255.

4 Results

4.1 Invisibility and Information Decoding Efficiency

Figure 9 compares original and watermarked pictures with different content features. The resulting images have generally an acceptable quality, the pictures of Demi and Lena in particular. However, the second picture (Boat) has lost some quality after embedding, especially near the edges (the masts). There is a wave effect in these areas that is visible on a good quality display or after high quality printing. This is the worst case for this method, which is still not perfect for embedding near sharp edges. Corrections brought about by edge detection and morphology still has to be improved in the future. Anyway, the quality of the watermarked picture is far from disastrous.

The analysis of retrieval tests revealed that the MLS phase is incorrect in only a few cases (Figure 10(a)). Moreover, some a priori knowledge may help to predict errors occurrence, since these mainly occur in regions with a high energy variance and energy mean value ratio(Figure 10(c)). An effective error detecting/correcting strategy has not been developed yet but it may be useful to locate an error once it has been detected, e.g. through error detecting



(a.1)



(a.2)



(b.1)



(b.2)



(c.1)

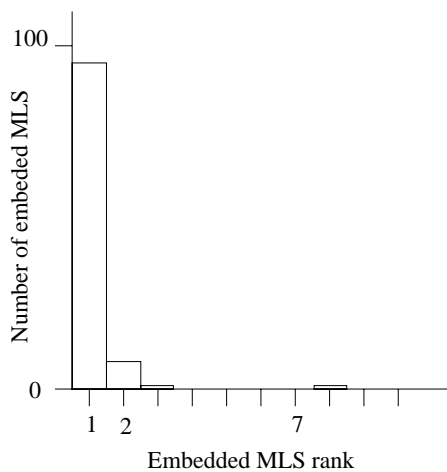


(c.2)

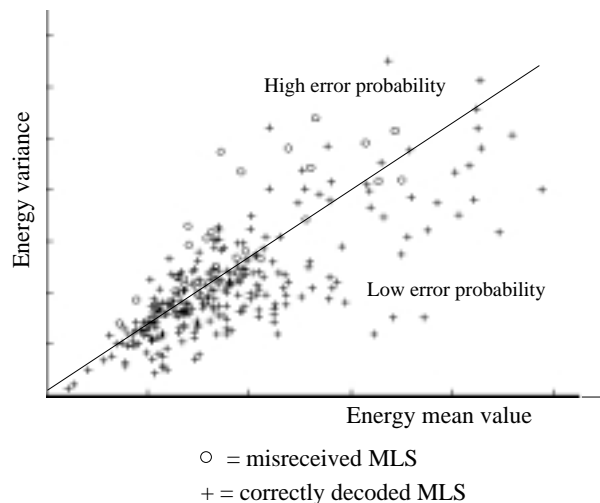
Fig. 9. Invisibility verification for (a) Lena, (b) Boat, (c) Demi: (1) original picture, (2) watermarked picture.

Picture	Lena	Boat	Demi	Average
Bit Error Rate (%) (Misreceived sequences number)	1.8	3.0	2.4	2.6

(a)



(b)



(c)

Fig. 10. Decision step effectiveness: (a) error rate (= number of MLS incorrectly decoded), (b) Histogram of the rank of the embedded MLS reception in the decreasing ordered list of the reception values generated by all the shifted versions of the MLS, (c) errors occurrence in an energy variance versus energy mean graph.

codes [30]. Finally, figure 10(b), shows that when an error occurs, i.e. there exists a shifted MLS giving a greater correlation value than the one obtained by correlation with the really embedded MLS, the correct phase may be recovered simply by taking the sequence having the second correlation value. The addition of a simple BCH code would still allow to keep most of the 163 embedded bits for the actual copyright information.

The watermarking method has also been applied on a database of 40 images having very different content features. These images are ranging from very textured images to images containing a lot of edges. The average retrieval bit error rate is shown in the last column of (Figure 10(a)).

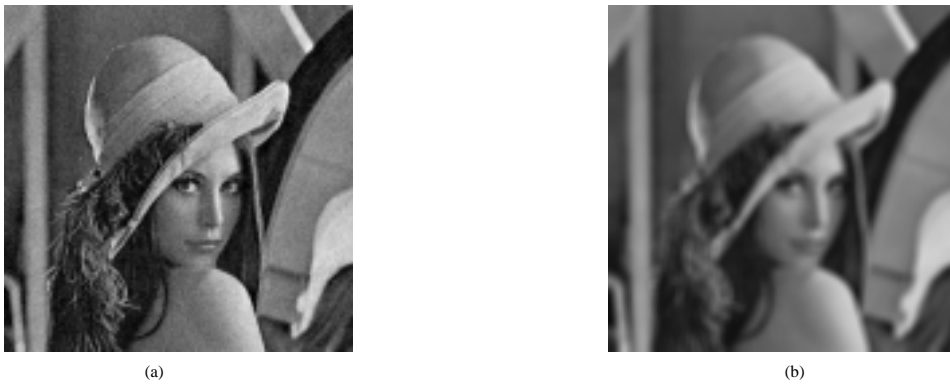


Fig. 11. (a) Lena with addition of white noise (b) Lena blurred with a 7x7 filter.

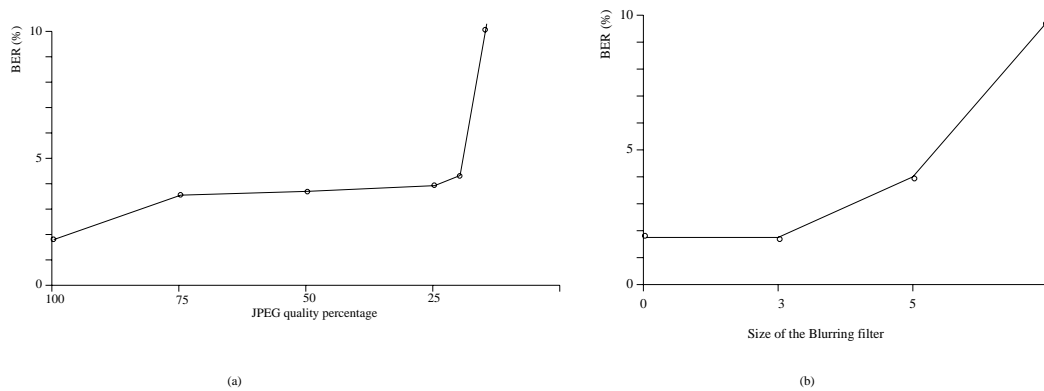


Fig. 12. (a) Evolution of the BER regarding the JPEG quality percentage, (b) Evolution of the BER regarding the size of the blurring filter.

4.2 System Robustness

4.2.1 Noise

Resistance to white noise is a minimal requirement that both methods fulfill. This is due to the correlative approach for the retrieval. The noise, whose variance is 100dB has nearly no influence on the detection. The BER for the retrieval tried on Lena has the same value as the retrieval without noise, i.e. 1.8%. Figure 11.a is the picture of Lena altered by the addition of white noise (variance 100dB).

4.2.2 JPEG [31] and Low-Pass Filtering

Resistance against lossy compression is essential to a watermarking method. Actually, a great part of the digital pictures that are exchanged on digital networks are compressed. What is more, it would be very simple to erase the watermark if it is not resistant against compression. The method presented in this paper reacts well to compression. Figure 12.a shows the evolution of

the bit error rate after retrieval regarding the JPEG quality percentage for the picture of Lena and for the images of the database used for the results of section 4.1. It appears that the compression does not significantly impede the retrieval, provided that the quality of the compressed picture is sufficient, i.e. above twenty percent. These positive results are not surprising because of the frequency range of the watermark. These frequencies are generally important for the original picture, whereas the compression algorithm removes the useless information. After comparing the results of the retrieval with and without compression, it seems that the error correcting code will allow dealing with compression without significantly diminishing the embedded bits of information. The same conclusion applies for resistance against low pass filtering, since the energy of the watermark is essentially concentrated in a frequency range where the image content is important. Figure 12.b illustrates the resistance against 3x3, 5x5 and 7x7 blurring filters. Figure 11.b is the picture of Lena altered by a 7x7 blurring filter.

4.2.3 Resistance Against Forgery

The most definitive attack consists in replacing the embedded watermark by a new one in favor of the pirate. This section analyzes the total number of possibilities available for embedding. It is essential to robustness against exhaustive attacks and overwatermarking. This is very important. It must be possible in practice to permit more than one watermark in the same image, without altering the previous ones too significantly. With this aim in mind, there must be enough independent positions for the watermark. The parameters of the embedding process include the choice of the MLS and the carrier frequency. As far as the carrier frequency is concerned, about one hundred frequencies are available in the interval $[0.1, 0.2]$ of the normalized frequencies, because carriers having a $\Delta f_{normalized} \geq \frac{0.1}{100}$ can be considered orthogonal on the length of an MLS. Moreover, for each embedded MLS, one can choose a different carrier. There are 33 embedded MLS. There are thus 100^{33} , i.e. 2^{220} possibilities to choose the embedding parameters. This number is huge but does not represent the actual system robustness against a pirate because the analysis of the decoding correlations obtained by decoders tuned on 100 distinct frequencies and the 186 possible MLS may convey information about the parameters used due to the appearance of particular peak features in the correlation. Nevertheless, due to his ignorance of the synchronization bits, the pirate is confronted with a strong phase acquisition problem: "How to choose the phase of the MLS carrier during the retrieval process?". It is noticeable that the very high noisy channel features prevents the pirate from using a classical *Phase Locking Loop*. The same positive conclusion can be made for overwatermarking. If someone adds another watermark without any a priori knowledge of the frequencies used for the first one, he will use the same frequencies for one percent of the MLS on average. When this occurs, half the MLS bits will be altered, the other half will be more strongly embedded. This

will produce an average percentage of 0.5 errors on the whole image during retrieval.

5 Conclusion

The main asset of the method presented in this paper is the use of a visual perceptive model in the production of an invisible watermark. The results are encouraging, even if in a few cases some drawbacks in the embedding method and the model itself appear. Further research would most probably solve these occasional problems. Moreover, this method reveals some interesting properties, such as the possibility of synchronization. The results seem encouraging. The bit error rate after retrieval is very low, so that an adapted error correcting code would permit keeping a great part of the 163 embedded bits for copyright information. The resistance against lossy compression and overwatermarking are other very good results and can easily be dealt with by the above mentioned error correcting code.

References

- [1] B. Kahin. The Strategic Environment for Protecting Multimedia. *IMA Intellectual Property Proceedings*, 1:1–8, January 1994.
- [2] K. Matsui and K. Tanaka. Video-Stenography: How to embed a Signature in a Picture. *IMA Intellectual Property Proceedings*, 1(1):187–205, January 1994.
- [3] J.T. Brassil, S. Low, N.F. Maxemchuk, and L. O’Gorman. Electronic Marking and Identification Techniques to Discourage Document Copying. *Proceedings of IEEE INFOCOM’94*, pages 1278–1287, June 1994.
- [4] W. Bender, D. Gruhl, and N. Moromoto. Techniques for Data Hiding. *Proceedings of the SPIE*, 2420(40), February 1995.
- [5] O. Bruyndonckx, J.J. Quisquater, and B. Macq. Spatial Method for Copyright Labelling of Digital Images. *Proceedings of IEEE Workshop on Non-Linear Processing*, pages 456–459, June 1995.
- [6] G. Caronni. Assuring Ownership Rights for Digital Images. *Proceeding of Reliable IT Systems, VIS 95*, June 1995.
- [7] I.J. Cox, J. Kilian, T. Leighton, and T. Shamoan. Spread Spectrum Watermarking for Multimedia. *Proceedings of the SPIE*, 2420:456–459, February 1995.
- [8] E. Koch and J. Zhao. Towards Robust and Hidden Image Copyright Labeling. *Proceedings of IEEE Workshop on Non-Linear Processing*, pages 452–455, June 1995.

- [9] B. Macq and J.J. Quisquater. Digital Images Multiresolution Encryption. *The journal of the Interactive Multimedia Association Intellectual Property Project*, 1:187–206, January 1994.
- [10] J. J. K. O’Ruanaidh, W. J. Dowling, and F. M. Boland. Phase watermarking of images. pages 239–242, Lausanne, Switzerland, September 1996. IEEE International Conference on Image Processing.
- [11] J.F. Delaigle, C. De Vleeschouwer, and Macq B. Digital Watermarking. In *Conference 2659 - Optical Security and Counterfeit Deterrence Techniques*, San Jose, February 1996. SPIE Electronic Imaging: science and technology. pp. 99-110.
- [12] G.W. Braudaway, K.A. Magerlein, and F. Mintzer. Protecting Publicly Available Images with a Visible Image Watermark. In *Conference 2659 - Optical Security and Counterfeit Deterrence Techniques*, San Jose, February 1996. SPIE Electronic Imaging: science and technology. pp. 126-133.
- [13] S. Comes. *Les traitements perceptifs d’images numérisées*. PhD thesis, Université catholique de Louvain, June 1995.
- [14] John Wiley, L.A. Olzak, and J.P. Thomas. *Handbook of Perception and Human Performance. Volume 1: Sensory Processes and Perception. Chapter 7: Seeing Spatial Patterns*. University of California, Los Angeles, California, 1986.
- [15] G.E. Legge. Spatial Frequency Masking in Human Vision: Binocular Interactions. *J. Opt. Soc. Am. A*, 69(6):838–847, June 1979.
- [16] H.R. Wilson, D.K. McFarlane, and G.C. Phillips. Spatial Frequency Tuning of Orientation Selective Units Estimated by Oblique Masking. *Vision Research*, 23(9):873–847, 1983.
- [17] H.R. Wilson and G.C. Phillips. Orientation Bandwidths of Spatial Mechanisms Measured by Masking. *J. Opt. Soc. Am. A*, 1(2):226–232, February 1984.
- [18] R.J. De Valois, D.G. Albrecht, and L.G. Thorell. Spatial Frequency Selectivity of Cells in Macaque Visual Cortex. *Vision Research*, 22:545–559, 1982.
- [19] J.J. Kulikowski and P.O. Bishop. Fourier Analysis and Spatial Representation in the Visual Cortex. *Experientia*, 37:160–163, 1981.
- [20] M.A. Webster and R.L. De Valois. Relationship between spatial frequency and orientation tuning of striate cortex cells. *J. Optical Soc. Am.*, A2(7), July 1985.
- [21] J. Daugman. Uncertainty Relation For Resolution In Space, Spatial Frequency, And Orientation Optimized By Two-dimensional Visual Cortical Filters. *J. Opt. Soc. Am. A*, 2(7):1160–1169, July 1985.
- [22] John G. Proakis, editor. *Digital Communications*, chapter 4, pages 152–232. McGRAW-HILL INTERNATIONAL EDITIONS, 1995. ISBN 0-07-113814-5.
- [23] I. Daubechies. The Wavelet Transform, Time-Frequency Localization and Signal Analysis. *IEEE Transactions on Information Theory*, 36(5):961–1004, 1990.

- [24] Tai Sing Lee. Image Representation Using 2D Gabor Wavelets. *IEEE Transactions on Pattern Analysis and Machine Intelligence*, 18(10):959–971, October 1996.
- [25] D.V. Sarwate and Pursley M.B. Crosscorrelation Properties of Pseudorandom and Related Sequences. *Proceedings of the IEEE*, 68(5):593–617, May 1980.
- [26] Ray H. Pettit. Codes for Spread Spectrum. In *ECM and ECCM Techniques for Digital Communication Systems*, chapter 3, pages 37–60. Lifetime Learning Publications, Belmont California.
- [27] A.N. Netravali and B.G. Haskell. Visual Psychophysics. In *Digital Picture: Representation and Compression*, chapter 3. Plenum Press, New-York, 1988.
- [28] S. Venkatesh and R. Owens. Implementation Details of a Feature Detection Algorithm. Technical Report 89/12, Department of Computer Science, University of Western Australia, 1989.
- [29] R.M. Haralick, S.R. Sternberg, and X. Zhuang. Image Analysis Using Mathematical Morphology. *IEEE Transactions on Pattern Analysis and Machine Intelligence*, 9(4):532–550, July 1987.
- [30] M. Purser. *Introduction to Error Correcting Codes*. Artech House, Boston-London, 1995. ISBN 0-89006-784-8.
- [31] G.K. Wallace. The jpeg still picture compression standard. *Communications of the ACM*, 34(4):30–44, April 1991.